A type IVB secretion system adapted for bacterial killing, biofilm invasion and biocontrol

Gabriela Purtschert-Montenegro
Department of Plant and Microbial Biology, University of Zurich
Gerardo Cárcamo-Oyarce
Massachusetts Institute of Technology
Marta Pinto-Carbó
Department of Plant and Microbial Biology, University of Zurich
Kirsty Agnoli
Department of Plant and Microbial Biology, University of Zurich
Aurelien Bailly
Department of Plant and Microbial Biology, University of Zurich
Leo Eberl (leberl@botinst.uzh.ch)
Department of Plant and Microbial Biology, University of Zurich https://orcid.org/0000-0002-7241-0864

Article

Keywords: type IVB secretion system, Pseudomonas putida IsoF, bacterial killing, biofilm invasion, biocontrol

Posted Date: October 22nd, 2021

DOI: https://doi.org/10.21203/rs.3.rs-959170/v1

Version of Record: A version of this preprint was published at Nature Microbiology on September 19th, 2022. See the published version at https://doi.org/10.1038/s41564-022-01209-6.

A type IVB secretion system adapted for bacterial killing, biofilm invasion and biocontrol

Authors: Gabriela Purtschert-Montenegro[1†], Gerardo Cárcamo-Oyarce[1†#], Marta Pinto-Carbó[1], Kirsty Agnoli[1], Aurélien Bailly[1] and Leo Eberl[1*]

Affiliations

[1] Department of Plant and Microbial biology, University of Zurich, Zurich, Switzerland

[†]These authors contributed equally to this work

[#]Current addresses: Department of Biological Engineering, Massachusetts Institute of Technology, Cambridge, Massachusetts, USA.

*Correspondence to: leberl@botinst.uzh.ch

Abstract

Many bacteria utilize contact-dependent killing machineries to eliminate rivals in their environmental niches. Here, we show that *Pseudomonas putida* IsoF is able to outcompete a wide range of bacteria with the aid of a novel type IVB secretion system (T4BSS) that can deliver toxic effectors into bacterial competitors. This extends the host range of T4BSSs, which were so far thought to transfer effectors only into eukaryotic cells, to prokaryotes. Bioinformatic and genetic analyses showed that this killing machine is entirely encoded by a rare genomic island, which has been recently acquired by horizontal gene transfer. IsoF utilizes this secretion system not only as a defensive weapon to antagonize bacterial competitors but also as an offensive weapon to invade existing biofilms, allowing the strain to persist in its natural environment. Furthermore, we show that IsoF can protect tomato plants against the plant pathogen *Ralstonia solanacearum* in a T4BSS-dependent manner, suggesting that IsoF capabilities can be exploited for pest control and sustainable agriculture.

Introduction

Many reports have demonstrated the great potential of microbial inoculants for bioremediation, biofertilization and biocontrol applications[1–4]. However, the lab-to-field transition remains a major limiting factor, since good *in vitro* performance is rarely reproduced in field trials. Microbial survival, establishment and colonization are key features for biocontrol agents and applied microorganisms were often unable to persist in the environment or are rapidly outcompeted[5–7]. Despite decades of research, the lack of understanding of intricate polymicrobial interactions has hampered the widespread use of inoculants in sustainable agriculture[8–11]. One important reason for the failure of a strain to colonize a desired niche is that the planktonic inoculants are unable to invade and persist in indigenous microbial consortia, which live within surface-associated communities, commonly referred to as biofilms[5,12–15]. Biofilm cells are embedded in an extracellular matrix that protects them from external stresses, like nutrient limitation, predation and the host immune response[12,13,16,17]. The extracellular matrix also restricts the entry of invaders into the biofilm interior and while bacteria can colonize and grow on the biofilm exterior, they are readily removed by shear forces[18]. Moreover, the ability to form biofilms is a widespread trait in plant-associated bacteria, that allows them to maintain a critical population in a specific location for periods sufficient to initiate beneficial or antagonistic interactions with the host plant[19,20].

In addition, members of the indigenous biofilm consortium have evolved an arsenal of defense strategies[21] that limit the successful establishment of inoculants in the rhizosphere. Bacteria display two main strategies to antagonize invaders: the release of small molecules with antimicrobial activity into their surroundings[22] and the delivery of toxic effector proteins through secretion systems into neighboring opponents, which relies on cell-to-cell contact[23]. Some of these effector molecules cause cell lysis by disrupting the cell envelope, while others are delivered into the cytoplasm where they affect DNA integrity or cell division, or exhaust energy resources[24–30]. To avoid self-intoxication by the effectors, bacteria produce cognate immunity proteins, which are typically encoded by a gene localized in the vicinity of the effector gene[23,31,32]. Various secretion systems are known to deliver effector proteins into bacterial competitors[23,31,33]. The type V secretion systems (T5SS), encoded by the *cdiBAI* gene cluster,

are widespread in Gram-negative bacteria. CdiB is an outer membrane β-barrel protein that exports the toxic CdiA protein, which forms a long filament extending from the cell surface. Upon binding of CdiA to specific receptors on the target cell, the C-terminal toxin domain is delivered into the bacterium to inhibit growth[34,35]. In *Caulobacter crecentus*, a type I secretion system (T1SS) exports the two bacteriocin-like proteins CdzC and CdzD to the surface of the producer cell where they form insoluble aggregates. These aggregates can drive contact-dependent killing of competitors by creating pores in the inner membrane[25,31]. The most versatile weapon, deployed by 25% of all Gram-negative bacteria, to target rival bacteria is the type VI secretion system (T6SS)[36]. It employs a contractile, phage-related nanomachine composed of several protein subcomplexes to inject diverse effectors into target cells in a one-step manner[36–38]. Most recently, a type IV secretion system (T4SS) was identified in *Xanthomonas citri* that is used to deliver an effector with peptidoglycan (PG) hydrolase activity, which lyses susceptible competitor cells[26,31]. There are two main classes of T4SS: i) The type IV A secretion systems (T4ASS), mostly used for DNA delivery and exemplified by the VirB/D4 system of *Agrobacterium tumefaciens*, and ii) the type IV B secretion systems (T4BSS), utilized to deliver effector proteins into their eukaryotic hosts and initially described as the Dot/Icm system found in intracellular pathogens such as *Legionella pneumophila* [39–42]. The two classes are only distantly related and T4BSS assemblies are larger than T4ASSs, comprising 27 components for the *L. pneumophilla* Dot/Icm system compared to 12 components for the VirB/D4 system[42].

In this study, we identified a T4BSS that can deliver toxic effectors into bacterial competitors, breaking the paradigm that T4BSSs are only used for effector transfer into eukaryotic cells[43,44]. This novel bacterial killing machine is encoded by a rare genomic island that was probably horizontally acquired by *Pseudomonas putida* IsoF, which is an effective colonizer of plant roots[45,46]. We demonstrate that IsoF utilizes this secretion system not only as a defensive weapon to antagonize phylogenetically diverse bacterial competitors but also as an offensive weapon to invade an existing biofilm by contact-dependent killing. We also show that IsoF can protect tomato plants against the pathogen *R. solanacearum* in a T4BSS-dependent manner, suggesting that this killing machine can be exploited for pest control.

Results

IsoF exhibits contact-dependent antagonism against a wide range of Gram-negative bacteria

We observed that *P. putida* IsoF (marked with Gfp; IsoF::Gfp) inhibited the growth of *P. putida* KT2442 (marked with mCherry; KT2442::mCherry) when culture samples were inoculated in a 1:1 ratio on a minimal medium plate. After 24 hours in contact-dependent competition (CDC), no red fluorescence could be observed from the macrocolony, indicating that the KT2442 had been outcompeted. We next determined the CFUs of the two strains after 24 h and 48 h and found that after two days IsoF had completely eliminated KT2442 (Fig. 1a). No adverse effect was seen when the two strains were separated by a 0.2 μm pore size filter, suggesting that killing depends on cell-to-cell contact (Extended Data Fig. 1). To obtain further insight into the underlying molecular mechanism, we performed competition experiments on plates supplemented with propidium idiode (PI), which allowed us to assess dead cells. After 48 hours of incubation, PI staining (magenta) was observed in the region where the two drops of the inoculated cultures overlapped, whereas dead cells were absent from the pure cultures regions (Fig. 1b). Time-lapse confocal laser scanning microscopy (CLSM) was used to demonstrate that KT2442 cells were killed after they had been in direct contact with IsoF::Gfp (Fig. 1c, Extended Data Video 1). We noticed that dead cells did not lyse or change their morphology.

To determine the host range of the antagonistic activity of IsoF we fluorescently marked several soil- and plant-associated bacteria as well as some phytopathogens, and tested whether they are susceptible to killing by IsoF. All tested strains were outcompeted after 24 h of co-culture with IsoF (Fig. 1d, e). Collectively, our data suggest that IsoF possesses a highly efficient, broad host-range, contact-dependent killing machinery.

IsoF utilizes a type IVB secretion system for bacterial killing

To identify the mechanism responsible for contact-dependent killing by IsoF, we constructed a mini-Tn*5* transposon insertion library of this strain and tested about 5,000 mutants for their ability to outcompete *P. aureofaciens*::mCherry when grown as mixed macrocolonies (Fig. 2a).

We identified 16 killing-defective insertion mutants (Extended Data Fig. 2). The transposon insertion sites of eight of these mutants were determined by arbitrary PCR[47] and were found to be located in four genes of a large gene cluster, which we designated *kib* (killing, invasion, biocontrol, see below), that appears to encode several elements of a T4BSS (Fig. 2b). While T4BSSs of intracellular pathogens are well known for their capacity to deliver effectors to their eukaryotic hosts[42,48,49], they have so far not been reported to be involved in interbacterial killing. To validate the results of the mutant screen, we constructed defined T4BSS mutants: Δ*dotHGF,* which lacks the main structural components of the secretion system channel and Δ23-*trbN-dotD,* which lacks *Piso_02323* encoding the hypothetical protein TrbN, which has a conserved transglycosylase domain that has been proposed to assist DNA transfer across the PG in conjugation systems[50]. The latter mutant also lacked DotD, encoding a lipoprotein required for assembly of the secretion system by positioning DotH in the outer membrane[51–53]. Single mutants of *Piso_02323* and *dotD* were also constructed and validated in CDC experiments. All mutants tested had lost their ability to outcompete *P. aureofaciens* (Fig. 2d) and KT2442 (Extended Data Fig. 3), demonstrating that inactivation of the T4BSS apparatus prevents IsoF from killing other bacteria.

The *kib* gene cluster is part of a unique genomic island present in only few *Pseudomonas* strains

The region comprising the *kib* locus has a GC content of 58.8 %, whereas the IsoF genome has an average GC content of 62.6 % (Extended Data Table 1), which suggests the *kib* locus is part of a genomic island that has been recently acquired by horizontal gene transfer. This hypothesis was further strengthened by analyzing the IsoF genome with ICEfinder, allowing the detection of mobile integrative and conjugative elements in bacteria[54]. This algorithm classified the IsoF genomic island containing *kib* as a putative conjugative element, since it contains T4SS-related genes and an integrase within the region. ICEfinder defined the borders of the gene cluster with genes *Piso_02313* and *intA_3*. Hence, the entire island has a size of 66,917 bp and encodes 61 genes, 17 of which share homology with described T4BSS structural genes, 37 were defined

as hypothetical proteins, and four encode a Type I Restriction Modification (RM) system and an integrase at the 3'-end of the island (Fig. 2b,c). The basic local alignment search tool (BLAST) was used to interrogate the cluster and revealed that *kib* genes are also present in 11 other *Pseudomonas* strains, 10 of which are environmental isolates and one is a clinical isolate. Eight of these strains were classified as *P. putida* (Extended Data Table 1). Interestingly, all orthologous *kib* gene clusters showed conserved synteny and were located at the same chromosomal position (Extended Data Fig. 4), suggesting a common ancestor. Notably, the orthologous clusters showed deletions at the 3'-end of the island, including the Type I RM system and the flanking integrase (Extended Data Figs. 4 and 5). Previous work has shown that the genes encoding components of T4BSSs are organized in smaller clusters that are distributed across the chromosome or plasmid of various bacteria[49]. In contrast, the *kib* locus appears to encode all components of the T4BSS and we were unable to identify additional genes potentially encoding other components of the secretion system in the genome of IsoF (Extended Data Fig. 5). These data reinforce the idea that the *kib* gene cluster has only recently been acquired *via* horizontal gene transfer and encodes all components of the bacterial killing machine.

The *kib* gene cluster encodes an effector-immunity (E-I) pair

Contact-dependent killing systems deliver toxic effector molecules into bacterial competitors. To avoid self-killing, the attacking bacterium produces a cognate immunity protein that neutralizes the toxin. The immunity and toxin genes form a so-called effector-immunity (E-I) pair, and are often co-transcribed[22,32,55,56]. The *kib* gene cluster does not contain any previously described or obvious candidate toxin genes but many hypothetical genes (Fig. 2b), which could potentially encode effector molecules. However, as effector proteins are very heterogeneous both in sequence and function[22,57], we were not able to identify promising candidates using *in silico* analysis. To investigate whether an E-I pair was present within the *kib* region, we deleted 49.5 kb of the genomic island containing all *kib* genes (*Piso_02313* to *Piso_02360,* Extended Data Fig. 5). The resulting mutant, designated ΔT4B, no longer killed *P. aureofaciens* and

formed mixed macrocolonies with this strain (Fig. 2d). Interestingly, the ΔT4B mutant became susceptible to KT2442 in co-culture on nutrient plates, likely because KT2442 possesses a T6SS that was shown to efficiently kill other bacteria[27] (Extended Data Fig. 3). Our original observation that IsoF kills KT2442 (Fig. 1a), suggests that *kib*-mediated killing is faster or more efficient than T6SS-mediated killing of KT2442. We hypothesized that the absence of an E-I pair would render the ΔT4B mutant sensitive to the wild type strain, while its presence would confer resistance. In competition experiments between IsoF and ΔT4B, the mutant strain was indeed killed, while it was able to co-exist with the Δ*dotHGF* mutant, which lacks the structural components of the secretion channel required for killing (Fig. 3a). These experiments demonstrate that the genes required for killing and self-protection are present within the *kib* cluster. Moreover, IsoF was unable to kill mutants Δ*dotHGF* and Δ*23-trbN-dotD*, indicating that both deletion mutants are protected against effector toxicity from the wild type strain and that no immunity gene was located within the regions deleted in these mutants (Extended Data Fig. 6).

Identification of a *kib* immunity protein through transposon sequencing

Immunity genes are essential since cells lacking an immunity protein would either be killed by neighboring bacteria or die due to self-intoxication[32,58]. We therefore reasoned that it should be possible to identify the genetic elements required for self-protection by transposon sequencing. This approach has previously been employed to identify E-I pairs of T6SSs in *V. cholerae* and *P. aeruginosa*[58,59]. To this end, we generated a saturated transposon insertion library in the IsoF wild type strain. The pooled library, which consisted of approximately 700,000 mutants, was subjected to three different growth regimes: (i) growth in liquid medium with shaking to prevent cell-to-cell contact, (ii) growth on an agar surface either alone or (iii) in the presence of the competitor *P. aureofaciens* to promote competition (Fig. 3b). Sequencing of the genomic DNA resulted in more than 7 million reads per sample as summarized in Extended Data Table 2. We used the unique insertion density approach of the Tn-Seq explorer software to identify genes that provide a fitness benefit for growth under the different growth regimes[60]. This analysis

identified one gene, *Piso_02332*, within the *kib* region, which was virtually devoid of transposon insertions in all three treatments (Fig. 3c, Extended Data Table 3). This gene appears to be co-transcribed with *Piso_02333*, possibly constituting a novel E-I pair.

To determine the role of this putative E-I pair in bacterial killing, we deleted both genes in IsoF to generate Δ32-33. We were also able to delete the putative effector gene, giving rise to mutant Δ33. Unexpectedly, we noticed that the Δ32-33 grew slower on ABC minimal media relative to the parental strain or mutant Δ33 (Extended Data Fig. 8). In order to establish a fair competition situation despite the growth difference, the CDC assays with Δ32-33 were performed on ABC medium supplemented with casamino acids and the CFUs were normalized to the number of cells recovered from the monoculture of Δ32-33 after 24 h. Importantly, Δ33 was unable to compete with *P. aureofaciens* or KT2442 and complementation partially rescued the killing phenotype, suggesting that *Piso_02333* encodes a toxic effector protein. This is further supported by the lack of growth inhibition of *P. aureofaciens* and KT2442 by the double mutant Δ32-33, although we were unable to restore killing by complementation (Extended Data Fig. 9a, b). In competition against IsoF wild type, mutant Δ33 and its complemented derivative survived (Fig. 3d), indicating that both strains are immune to the IsoF effector toxin. By contrast, mutant Δ32-33 was outcompeted by IsoF, while the complemented strain co-existed with IsoF (Fig. 3d), indicating that *Piso_02332* confers immunity to *kib*-mediated killing. To further test this possibility, mutants ΔT4B and Δ32-33 were complemented with *Piso_02332* on a plasmid (pBBR::32) and the resulting strains were used in competition assays against IsoF. While strain Δ32-33/pBBR::32 co-existed with IsoF, mutant ΔT4B/pBBR::32 was outcompeted (Fig. 3e). This suggests that while *Piso_02332* confers resistance to *Piso_02333*, *kib* may encode an additional effector that is not neutralized by *Piso_2332.*

The *kib* killing system enables IsoF to invade an established biofilm

We hypothesized that contact-dependent competition might be an efficient way to eliminate competitors in communities such as polymicrobial biofilms. Since both IsoF and KT2442 are good biofilm producers, they represent a good proxy for evaluating the role of *kib*-mediated

competition in mixed-species biofilms. To investigate this, we first established a KT2442::Gfp (green) biofilm in a flow cell system and then introduced IsoF::mCherry (blue) (Fig. 4a). Within one day, IsoF cells attached to the surface began to proliferate and formed numerous microcolonies. After 3 days of incubation IsoF had formed a mature biofilm by invading and displacing the KT2442 biofilm. The volume of KT2442 biofilm decreased by approximately 40 % between 72 and 96 h post IsoF inoculation, which reached the equal biomass with KT2442 after two days of competition (Fig. 4b). Without competition, the biomass of the KT2442 biofilm increased steadily over time (Extended Data Fig. 10a, b). When a pre-established KT2442 biofilm was challenged with the *kib* mutants Δ*dotHGF* or Δ23-*trbN-dotD*, neither of the mutants was able to form microcolonies or to invade the existing biofilm (Fig. 4a, b). Importantly, Δ*dotHGF* or Δ23-*trbN-dotD* mutants in isolation formed biofilms similar to the IsoF wild-type strain (Extended Data Fig. 11a, b). We hypothesized that IsoF employed its T4BSS to kill KT2442 cells upon contact within the biofilm, creating space for the expansion of the IsoF biofilm. To test this, we inoculated flow cells with IsoF::Cfp (cyan) and KT2442::Gfp (yellow) with equivalent numbers of cells and monitored the fate of KT2442 microcolonies neighboring IsoF microcolonies by adding PI (red) as an indicator of cell death. As shown in Figure 4e, dead cells were observed at positions where the two strains were in direct contact. We determined that the biofilm volume of KT2442 was reduced by approximately 20 % (Fig. 4f). We next visualized killing of KT2442 by IsoF::Gfp in a mixed monolayer biofilm on the surface of a minimal medium agar pad (Fig. 4c). After 18 h incubation we observed that nearly 92 % of the dead KT2442 cells present (magenta) were located next to IsoF::Gfp (green) cells, as opposed to those that were not in contact with a green cell, demonstrating that *kib*-mediated killing is strictly dependent on cell-to-cell contact (Fig. 4d). By contrast, when KT2442 was challenged with either the Δ*dotHGF* or the Δ23-*trbN-dotD* mutant (green), very few dead cells were observed, similar to monoculture biofilm controls (Fig. 4d, Extended Data Fig. 12). In conclusion, these results suggest that the *kib* system not only allows IsoF to defend itself against competitors but also to kill bacteria that live within an established biofilm community, which eventually becomes replaced by the biofilm of the invading IsoF strain.

Kib-mediated killing allows IsoF to protect tomato plants from the phytopathogen *Ralstonia solanacearum*

Since IsoF was initially isolated from the rhizosphere of tomato plants and was shown to efficiently colonize the root surface[46], we assessed whether the *kib* killing system could be useful for the biocontrol of *R. solanacearum,* a major pathogen causing bacterial wilt in tomato, amongst a wide range of other crops[61,62]*. In vitro* competition experiments showed that IsoF outcompeted *R. solanacearum,* while the ΔT4B mutant did not (Fig. 1d, e, Extended Data Fig. 13). We next tested whether IsoF could also protect tomato plants from *R. solanacearum* infection. Considering that *R. solanacearum* is a soil-borne pathogen which enters the plant through natural openings like emerging lateral roots or wounds[61], we injured established tomato seedlings with small incisions (Fig. 5a). Twenty-two days post infection, control plants inoculated with *R. solanacearum* were severely wilted, with signs of chlorosis and arrested development of the root and shoot systems. By contrast, 90% of the seedlings inoculated with a mixture of *R. solanacearum* and IsoF showed no signs of wilting (Fig. 5b). However, when seedlings were co-inoculated with a mixture of *R. solanacearum* and the *kib* mutant ΔT4B, wilting and underdevelopment were observed in 85% of the plants, indicating that IsoF prevented *R. solanacearum* from spreading into the plant tissues by *kib*-mediated killing. To precisely evaluate wilt development, we determined the chlorophyll content and measured shoot area and root weight of individuals from the treatment groups as a proxy for plant health. These data were subjected to principal component analysis and hierarchical clustering (Fig. 5b, c). The two first components accounted for 94.6 % of the variance and a score scatter plot clearly clustered the single inoculations with IsoF and ΔT4B groups together with untreated plants, confirming that the strains do not harm tomato plantlets. Plants co-inoculated with *R. solanacearum* and IsoF preferentially clustered with healthy plants while those co-inoculated with ΔT4B grouped with *R. solanacearum* infected plants. This clearly indicates that IsoF decreases the pathogen load in the injured tomato tissues in a *kib*-dependent manner. To verify that IsoF indeed killed *R. solanacearum,* we recovered the bacteria attached to the roots and

281 determined the CFUs. This showed that the number of *R. solanacearum* cells present after co-
282 inoculation with IsoF was significantly lower than after inoculation with the ΔT4B mutant (Fig.
283 5d). Together, these results demonstrate that the biocontrol capacity of IsoF against bacterial
284 pathogens such as *R. solanacearum* depends on the *kib* locus.
285
286 **Discussion**
287 In this study, we show that *P. putida* IsoF uses a T4BSS to kill a wide range of soil and plant-
288 associated Gram-negative bacteria in a contact-dependent manner. This killing machinery
289 enables IsoF to invade and replace pre-established biofilms and to protect tomato plants from
290 the phytopathogen *R. solanacearum*. Consequently, we have named the gene cluster encoding
291 this T4BSS *kib* (killing, invasion and biocontrol). While previous work has demonstrated that the
292 opportunistic pathogen *Stenotrophomonas maltophilia*, the plant pathogen *Xanthomonas citri*
293 and the animal pathogen *Bartonella schoenbuchensis* possess T4ASSs that kill other
294 bacteria[26,63,64], this is the first report of a T4BSS that is used for interbacterial killing. T4BSSs
295 are employed by various pathogens to translocate effector molecules into their eukaryotic host
296 cells[42,48,49] and thus *kib* extends the host range of T4BSSs to prokaryotes.
297
298 Our bioinformatic and molecular analyses showed that the *kib* locus encodes all components
299 of the killing machinery. This contrasts with other killing systems, where the genetic components
300 are often spread across the chromosome. For example, the loci encoding the structural genes
301 of the *Xanthomonas* and *Stenotrophomonas* T4ASSs are separated from the genes encoding
302 the effectors[63,65]. A similar separation has been reported for the *Legionella* T4BSS, which is
303 encoded in numerous clusters distributed over the entire genome and the plasmids[49,66]. Our
304 data suggest that *kib* is part of a genomic island and the striking difference in GC content
305 between the island and the IsoF core genome (4.6 %), together with the presence of genes
306 encoding an integrase as well as a Type I RM system flanking *kib,* suggest that it was recently
307 acquired by horizontal gene transfer (Fig. 2b, Extended Data Table 1). This is also in line with
308 the finding that orthologs of *kib* were only present in 11 *Pseudomonas* strains. Interestingly, all

309 of these homologous islands lacked the Type I RM system and the integrase (Extended Data
310 Fig. 5).
311
312 We speculated that the *kib* cluster provides IsoF a competitive advantage for survival in the
313 environment, as IsoF was shown to be an excellent colonizer of tomato roots and most of the
314 other strains carrying *kib* were also isolated from soil. Our results showed that IsoF indeed
315 outcompeted various environmental strains, most notably *P. putida* KT2442, which was recently
316 demonstrated to use its K1-T6SS as an antibacterial killing device[27]. IsoF does not harbor a
317 homolog of the K1-T6SS gene cluster and thus was expected to be sensitive to killing by
318 KT2442. In fact, the ΔT4B mutant of IsoF was found to be killed by KT2442 in co-culture.
319 However, when the two wild type strains were competed against each other, IsoF eliminated
320 KT2442, indicating that T4BSS-mediated killing may occur before KT2442 can fire its T6SS
321 apparatus (Fig. 1a, Extended Data Fig. 3). Previous work has shown that bacteria have different
322 strategies for deploying their T6SS. While some strains of *Vibrio cholerae* use their T6SS in an
323 untargeted fashion and assemble and fire their apparatus in random locations within the cell, *P.*
324 *aeruginosa* assembles and fires its organelle only after detecting an attack from another nearby
325 bacterium[67,68], a strategy that has been termed the T6SS tit-for-tat response[69]. More recent work
326 has provided evidence that *P. aeruginosa* senses outer membrane perturbations caused by the
327 attack of competitors, treatment with the membrane-targeting antibiotic polymyxin, or
328 interference with outer membrane biogenesis *via* a signal transduction pathway that triggers
329 the tit-for-tat response[70]. At present, neither the triggers of the KT2442 K1-T6SS nor of the IsoF
330 *kib* system are known. However, that IsoF kills KT2442 may indicate that *kib* is constitutively
331 expressed and fires in a random fashion, while the K1-T6SS of KT2442 is only activated upon
332 attack. This would be reminiscent of the finding that a T6SS-negative *V. cholerae* strain is not
333 killed by *P. aeruginosa* whereas *V. cholerae* is efficiently killed in co-cultures with *P. aeruginosa*
334 when both organisms contain a functional T6SS[69]. While this would explain why all defined *kib*
335 mutants of IsoF co-existed with KT2442, it does not explain why the ΔT4B mutant, which lacks
336 the entire *kib* locus, was killed by KT2442. Additional work will be required to elucidate whether

differences in the triggers or efficacies of the killing systems are responsible for the superior performance of the IsoF *kib* system. In this context, it is worth noting that IsoF killed many bacteria that were shown to use T6SSs for interbacterial competition, including *P. aeruginosa* PA14[27], *B. cenocepacia* H111[71], *P. syringae*[72], *P. chlororaphis*[73], *P. fluorescens*[74], *P. carotovorum*[75], *E. amilovora*[76] and *B. thailandensis*[77] (Extended Data Fig. 14).

We performed a Tn-Seq analysis to identify potential E-I pairs within the *kib* gene cluster. This strategy, which assumes that inactivation of an immunity gene is lethal for the cell, identified *Piso_02332* as an essential gene. Importantly, we found this gene to be essential for growth under all conditions tested, namely in liquid medium, in a macrocolony on the surface of an agar plate or in the presence of a competitor strain, suggesting that this gene is constitutively expressed. We provided evidence that *Piso_02332* encodes an immunity protein that neutralizes the toxicity of an effector protein encoded by *Piso*_02333, which appears to be co-transcribed with Piso_02332, a genetic architecture that is frequently found with E-I pairs[22,32,55,56]. A defined *Piso_02333* mutant killed neither KT2442 nor *P. aureofaciens* and this defect was at least partially restored by genetic complementation (Extended Data Fig. 9). At present the cellular target of the Piso_02333 effector is unknown. Given that cells killed by IsoF maintained their shape and did not lyse, it is tempting to speculate that the target is located in the cytosol rather than the cell envelope. Expression of Piso_02332 in the Δ32-33 mutant conferred immunity against the IsoF wild type strain, indicating that Piso_02332 neutralizes the toxicity of the Piso_02333 effector. Unexpectedly, complementation of ΔT4B, which lacks the entire *kib* locus, did not protect the mutant against IsoF, suggesting that an additional E-I pair may be encoded by the *kib* gene cluster (Fig 3e). We noticed that the transposon insertion density of another gene within the *kib* locus, *Piso_02351*, was reduced, albeit to a lesser degree than *Piso_02332* (Extended Data Fig. 7, Extended Data Table 3). Whether this gene together with one of its adjacent genes could comprise another E-I pair remains to be elucidated.

Natural biofilms have dynamic and heterogeneous structures that are shaped by both

environmental forces and microbial interactions, which may be cooperative or antagonistic[78–80]. The biofilm matrix protects the cells from various external stresses and restricts the entry of invaders into the biofilm[18,78]. Moreover, many bacteria use defense mechanisms that would effectively kill competitors that attempt to enter the established biofilm community[22,23,33]. In this study we demonstrate that *P. putida* IsoF has the unprecedented ability to invade and replace an established biofilm of *P. putida* KT2442. However, when the two wild type strains competed against each other, KT2442 was eliminated, presumably because it was killed before it could fire its T6SS. In accordance with a recent report[81], we observed that on agar plates dead cells created a barrier that prevented further killing. This was not observed when the biofilms were grown in flow cells, as dead KT2442 cells detached from the glass substratum and were removed by the shear forces of the nutrient flow. The freed space was then occupied by IsoF, which eventually led to the replacement of the existing KT2442 biofilm (Fig. 4a, b). It is worth mentioning that IsoF produces the powerful biosurfactant putisolvin, which was previously shown to promote surface translocation and biofilm expansion[82]. Whether putisolvin is involved in the removal of dead KT2442 cells or the movement of IsoF cells into the freed spaces in the KT2442 biofilm is another interesting topic for future investigations.

IsoF was originally isolated from the rhizosphere of a tomato plant and was shown to form a biofilm on root surfaces[83]. Here, we demonstrate that IsoF is able to antagonize several economically relevant phytopathogens (Fig. 1d, e). Moreover, we show that IsoF can protect tomato plants from the soil-borne pathogen *R. solanacearum*, which can infect over 250 different plant species, among them important agricultural crops[61] (Fig 5). The presence of microbes secreting bacteriocins, antifungals or antibiotics in the rhizosphere was shown to be an effective strategy to suppress plant pathogens[21,80,84]. In this study we demonstrate that IsoF uses its T4BSS not only to kill phytopathogens but also to invade biofilms. Given that a major limitation in biocontrol applications is that inoculants are unable to establish themselves in the environment, IsoF, which utilizes *kib* for attack as well as for defense, is a very strong candidate for a novel bioinoculant for plant protection.

Methods

Bacterial growth conditions and media

Bacterial strains used in this study have been listed in Table 1. Most bacterial overnight cultures were grown in Lysogeny Broth (LB, Difco) at 30°C (*Pseudomonas* species) or at 37°C (*Escherichia coli*). *Ralstonia solanacearum*, *Pectobacterium carotovorum, Pseudomonas syringae* overnight cultures and experiments were done in LB media without salt (LB-, Difco) at 30°C. All other experiments were performed in AB medium[85] supplemented with 10 mM sodium citrate (indicated as ABC medium). If indicated, ABC was supplemented with 4 μg ml^{-1} propidium iodide (PI, Thermo Fisher). Additionally, ABC was supplemented with 0.2% casamino acids if indicated (ABCAS). For selection of *Pseudomonas* mutants or transconjugants, Pseudomonas Isolation Agar (PIA, Difco) was used. If required, antibiotics were added at the following final concentrations: for *E. coli*: 100 μg ml^{-1} ampicillin (Amp), 25 μg ml^{-1} kanamycin (Km), 10 μg ml^{-1} gentamycin (Gm), 10 μg ml^{-1} tetracycline (Tc); for *Pseudomonas* species: 75 or 100 μg ml^{-1} kanamycin, 20 or 30 μg ml^{-1} gentamycin, 20 μg ml^{-1} tetracycline.

Construction of fluorescently tagged strains

The mini-Tn*7* system[86] was employed to integrate the gene encoding red fluorescent protein (mCherry) or green fluorescent protein (Gfp), into the chromosome of the strains listed in Table 1. Mini-Tn*7* tagged strains were obtained by tri-parental mating using the donor strain *E. coli* S17-1 carrying pUCT18-mini-Tn*7* and the helper plasmid pUX-BF13[87]. Briefly, overnight cultures of the recipient strain, the helper strain and the donor strain were washed with 0.9% NaCl and then mixed in a 1:2:2 ratio (recipient : helper : donor). The strains were inoculated on LB plates as 50 μl drops and incubated at 30°C overnight. Bacteria were resuspended in 1 ml 0.9% NaCl and plated on media containing Gm. Plates were incubated overnight at 30°C and fluorescent colonies were selected.

Tn*5* mutant library, screening and mutant identification

A transposon mutagenesis was performed as previously described[88,89] , using IsoF as the genetic background and the transposon delivery vector pUT/mini-Tn*5* Km[90]. Approximately 40,000 independent transposon insertion mutants were obtained. Aliquots of the library were saved and stored at -80°C. To perform the screening, individual mutants were grown overnight in 100 µl LB on 96-well plates, then the cultures were gently combined with 100 µl of *P. aureofacien*s::mCherry. The mixed- inocula were transferred to ABC medium agar plates using a 96-pin replicator. Approximately 5,000 single Tn*5* mutants were independently co-inoculated with *P. aureofacien*s::mCherry and incubated for 24 h at 30°C. Mixed bacterial colonies were examined by means of fluorescence microscopy where competitions that showed red fluorescence indicated Tn*5* mutants defective in killing. Initial hits were validated by contact-dependent competition assays as described later. Identification of the Tn*5* insertion mutants was done by arbitrary PCR as described by Espinosa-Urgel et al, 2000[47]. After the second round of PCR, reactions were cleaned with the PCR Purification Kit (Qiagen) and sequenced. Sequences were analysed and compared with the genome of IsoF and with NCBI Blast. The whole genome sequence of IsoF has been uploaded and is publicly available on NCBI under the accession number CP072013.

Contact-dependent competition (CDC) assays

Overnight cultures were adjusted to an OD_{600} of 1 and dilutions were made to determine the number of colony forming units (CFUs) of each competitor. For the CDC assays, competitors were mixed in a 1:1 CFU ratio. ABC, ABCAS, or LB medium was inoculated with 5 µl of mixed culture. To determine the bacterial population in the mixed macrocolonies, CFU were counted at 0 h and at 24 h. At 24 h, two macrocolonies were resuspended in 500 µl of 0.9% NaCl and serial dilutions were plated on PIA and PIA Gm, the latter to select tagged strains. For the macrocolony overlaying competition, IsoF::Gfp was inoculated first and incubated at 30°C for 1 h, then KT2442 was inoculated to cover half of the IsoF colony. Fluorescence of the mono and mixed cultures was examined using a Leica M165 FC Fluorescence Stereo Microscope.

449

450 **Single cell competitions**

451 On a microscope slide, 8-9 mm Ø x 1 mm depth adhesive silicon isolators (Grace BioLabs)
452 were attached and filled with 62 µl ABC with 0.7% agar supplemented with PI. The middle of
453 the agar was inoculated with 1 µl of the bacterial 1:1 mixed culture (IsoF::Gfp : competitor
454 strain). The cover slip was placed on top after the inoculant had dried, and competition was
455 monitored with a confocal laser scanning microscope every 15 min for about 3 h. A final time
456 point was recorded at after 18-22 hours of incubation at RT including samples of the mono
457 cultures. Image acquisition was done using a confocal laser scanning microscope (CLSM,
458 Leica TCS SPE, DM5500) equipped with a x100/1.44 oil objective. Images were analysed with
459 ImageJ[91].

460

461 **Construction of *P. putida* IsoF deletion mutants**

462 IsoF derivatives with single and triple gene deletions and the deletion of the *kib* cluster (49.5
463 kbp) were constructed using Sce-I based mutagenesis as described in Flannagan et al, 2008[92].
464 First, the plasmid pGPI-SceI (which carries an I-SceI recognition site) was modified by cloning
465 *tetAR,* which encodes a tetracycline efflux pump into the PstI restriction site to give pGPI-
466 SceI::TetAR. Next, two homology regions flanking the region to be deleted were cloned into
467 pGPI-SceI::TetAR. The plasmid was introduced via conjugation and integrated into the
468 genome of *P. putida* IsoF by single homologous recombination, giving two copies of the
469 homologous regions in the chromosome. The plasmid pDAI::Gm^R, which carries the I-SceI
470 nuclease, was then conjugated into the single-crossover IsoF strain. The I-SceI nuclease
471 produced a double strand DNA break at its recognition site, linearising the chromosome and
472 requiring recombination for the survival of the cell. This occurred preferentially at the repeated
473 homologous regions. For both conjugations, the pRK2013 helper plasmid was used to provide
474 the genes encoding the conjugation machinery. Ex-conjugants were selected on PIA Gm
475 plates and screened by PCR using the check primers. Colonies were patched on PIA and PIA

Gm20 to select colonies from which the pDAI plasmid had been cured. All primers and restrictions enzymes used for cloning are listed in Supplementary Table 2.

Construction of pBBR1MCS derivative plasmids

For complementation of the Δ32-33 and Δ33 mutants, plasmids pBBR::32-33 and pBBR::33 were constructed. Additionally, pBBR::32 was constructed. In each case the coding sequence plus the native promoter region was amplified using an IsoF cell lysate as a template and cloned into pBBR1MCS-2 using primers and restriction sites as listed in Supplementary Table 1 and 2. *E. coli* MC1061 was transformed with the ligated vectors, which were then transferred into the IsoF deletion mutants by triparental mating using *E. coli* DH5α pRK2013 as the helper strain. Complementation was checked by colony PCR using primers listed in Supplementary Table 2.

Comparative genomic analysis

Identification of *Pseudomonas* strains carrying the T4BSS gene cluster elements was performed using NCBI BLAST. The online tool ICEfinder was used to determine the boundaries of IsoF's genomic island (GI). The region containing the IsoF GI was compared against the 11 other *Pseudomonas* strains carrying T4BSS elements using the MAUVE alignment tool with the default settings[93]. MultiGeneBlast was done using the 11 *Pseudomonas* strains, IsoF, and 8 additional known species in which the T4BSS has been described[94]. Alignment and comparison were done using the following settings: Gene identity threshold 30%, number of hits mapped 1000 and maximum distance between the genes in a locus 10 kb to search for tightly coupled operons.

Tn-Seq methodology

Transposon mutagenesis was performed by tri-parental conjugation. First, the resistance properties of the donor plasmid pLG99 (carrying a Tn*23* transposon) were modified by cloning a kanamycin resistance gene into the AatII restriction site. Overnight cultures of the recipient

strain *P. putida* IsoF, the helper strain *E. coli* DH5α pRK2013 and the donor strain *E. coli* CC118 λ-pir pLG99::Km were washed with 0.9% NaCl and then mixed in a 1:2:2 ratio (recipient : helper : donor). The conjugation was plated on LB plates in drops of 50 μl and incubated for 2 h at 37°C, followed by incubation at 30°C overnight. The mating drops were resuspended in 6 ml 0.9% NaCl and plated on PIA containing Km. Plates were incubated at 30°C overnight and the resulting colonies were washed from the plate with LB supplemented with Km. The resuspended mutant library was then mixed with an equal amount of 50% glycerol and kept at -80°C. From three independent conjugations with approximately 70 matings, an estimated 700,000 mutants were generated.

For the Tn-Seq experiments, the pooled mutant library was first grown for 16 h in liquid ABC media supplemented with 0.2% rhamnose until stationary phase. The OD_{600} was then adjusted to 0.05 for growth in liquid medium (condition 1) and to an OD_{600} of 1 for growth on solid medium as a monoculture (condition 2) and on solid medium as a co-culture (condition 3). For the growth in liquid medium the Tn library was incubated at 30°C for 4.5 h with 220 rpm shaking, then cells were collected and pelleted for DNA extraction. For treatments 2 and 3, 400 drops of 5 μl each of the bacterial culture were plated. For the mixed condition (condition 3), *P. aureofaciens* was co-inoculated with the Tn mutant library in a 1:1 CFU ratio. Both plated conditions were incubated for 8.5 h at 30°C. Cells were scraped from the plate with 0.9% NaCl and adjusted to an OD_{600} of 2 before being pelleted and kept at -20°C for later DNA extraction. DNA extraction was done using the Bacterial Genomic DNA Kit (Sigma-Aldrich). All sequencing steps were performed using the circle method described by Gallager et al, 2011[95] with several modifications described in Higgins et al, 2020[96].

Tn-Seq data analysis and bioinformatics

The Illumina sequencing reads were trimmed using Trimmomatic-0.32 (Leading: 30, Trailing: 30, Slidingwindow: 4:20, Minlen: 60)[97]. Adapter sequences were removed with Cutadapt v1.9[98]. Tn-Seq Explorer was used to analyse the resulting Tn-Seq data[60]. NCBI protein (.ptt) and RNA (.rnt) table files were generated from the IsoF genbank file (.gbff) and provided as

input to Tn-Seq Explorer in order to infer the coordinates of proteins and RNA coding regions. Trimmed reads were mapped to the chromosome using the Bowtie 2 plugin of Tn-Seq explorer (--very-sensitive- command)[99]. A sequence alignment map (SAM) file was produced. For each dataset, the subsequent sequence alignment map (SAM) generated with Bowtie2 was evaluated by Tn-Seq Explorer to assess essentiality. In the analysis, transposons mapping within 5% of the start codon and 20% of the stop codon were excluded. An estimated cut-off UID (unique insertion density) was established in order to separate essential from non-essential genes[60]. This was done by dividing the number of unique insertions by the gene length, resulting in the UID for that specific gene. The number of genes with the given insertion density versus the insertion density per bp was represented in a plot, usually showing a bimodal distribution. Here the genes with low or no-insertions appeared on the left side of the plot. The point where the plot rises again indicates the threshold for genes that can tolerate transposon insertions[95]. This point indicates the cut-off for essential genes, which was set for each growth condition: Liquid = 0.013, Plate = 0.011 and Mixed = 0.014 (UID). Genes showing higher UID values were considered non-essential since high number of transposon insertions were detected per gene.

Availability of sequencing data

FASTQ files generated from the Illumina MiSeq platform are publicly available at the NCBI short reads archive (SRA) under the BioProject: PRJNA730700. Individual datasets have following accession numbers: Liquid: SRR14612110, Plate: SRR14612109 and Mixed: SRR14612108.

Flow-cell biofilms, microscopy and image analysis

Biofilms were grown in a flow cell system with continuous flow at a rate of 0.2 mm s^{-1} by a Watson-Marlow 205S peristaltic pump. The flow cell system was assembled as described previously[100] and liquid AB media supplemented with 0.1 mM sodium citrate was used[101]. Briefly, the flow cell chambers were inoculated with *P. putida* cultures at an OD_{600} of 0.1, biofilm

development was followed every 24 h up to 5 days. For the competition experiment, the strain inoculated on top of the pre-established biofilm was adjusted to an OD_{600} of 0.5. For the two-species biofilm, strains were mixed in a 1:1 ratio and cultivated for up to 48 h. Shortly before 40 h of cultivation, PI was added. Photomicrographs were taken every 24 h with a confocal laser scanning microscope (CLSM, Leica TCS SPE, DM5500) equipped with a 63 x 1.3 oil objective. Single cell competition assays were imaged with a 100 x 1.44 oil objective. Images were analysed with the Leica Application Suite, the Imaris 9.6.0 software package (Bitplane) and with ImageJ[91].

Plant assay

Micro-Tom *Solanum lycopersicum* L. seeds (Tuinplus bv. Heerenveen, Holland) were surface sterilized with 1% sodium hypochlorite solution for 10 min, washed 4 times with sterile dH_2O and placed at 4°C for 2 days in the dark. Seeds were then sown on 0.8% water agar plates and kept at 30°C for 2 days in the dark. Germinated seeds were incubated at 22°C in long day conditions (16 h light and 8 h dark, 100 uE, 60% RH) and seedlings were further grown for 6-7 days until lateral root emergence. Seedlings were injured twice with a 0.4 mm diameter needle at the root-shoot junction. The roots of the seedlings were then submerged for 10 seconds each in a bacterial suspension set to a final OD_{600} of 0.5 in 1 mM $MgSO_4$. Inoculated seedlings were next placed on half strength Murashige and Skoog (MS) medium with 1.5% agar and grown for 22 days under the long day conditions indicated above. Each tomato plant root was washed and sonicated as previously described[102] with the following modifications: roots were individually placed in an Eppendorf tube with 750 µl of 1 mM $MgSO_4$. The washing step consisted of shaking the tube for 15 min at 160 rpm, followed by sonication for 15 min. The obtained cell suspensions were serial-diluted to allow for CFU quantification. Principal component analysis and hierarchical clustering were performed on individual root weight, shoot area and chlorophyll values. Unit variance scaling was applied and SVD with imputation used to calculate PCs. Prediction ellipses were used to display the 95% confidence intervals. Root parameters were

clustered using correlation distance and average linkage, plant samples were clustered using Euclidean distance and average linkage. n = 144. Three independent biological replicates were performed with a total of 28 plants for each treatment. Shoot area and chlorophyll estimations were obtained from calibrated RGB photographs using Fiji[103] adapting previous methods[104]. Essentially, individual RGB values were extracted from Blue channel-thresholded plant pictures and normalized to total RGB. Normalized Green and Red channel values were used to calculate a greenness index (Greendex = 4G-3R). Greendex values and acetone-extracted total chlorophyll per shoot weight measured as previously described[105] of independent infected or healthy tomato plantlets were linearly correlated (R^2 = 0.7373, n=21).

References

1. Syed Ab Rahman, S. F., Singh, E., Pieterse, C. M. J. & Schenk, P. M. Emerging microbial biocontrol strategies for plant pathogens. *Plant Sci.* **267**, 102–111 (2018).
2. Berendsen, R. L., Pieterse, C. M. J. & Bakker, P. A. H. M. The rhizosphere microbiome and plant health. *Trends Plant Sci.* **17**, 478–486 (2012).
3. Prasad, M., Srinivasan, R., Chaudhary, M., Choudhary, M. & Jat, L. K. *PGPR amelioration in sustainable agriculture Ch. 7*. (Elsevier Inc., 2019).
4. Raymaekers, K., Ponet, L., Holtappels, D., Berckmans, B. & Cammue, B. P. A. Screening for novel biocontrol agents applicable in plant disease management – A review. *Biol. Control* **144**, 104–240 (2020).
5. Parnell, J. J. *et al.* From the lab to the farm: An industrial perspective of plant beneficial microorganisms. *Front. Plant Sci.* **7**, 1–12 (2016).
6. Hart, M. M., Antunes, P. M., Chaudhary, V. B. & Abbott, L. K. Fungal inoculants in the field: Is the reward greater than the risk? *Funct. Ecol.* **32**, 126–135 (2018).
7. Mitter, B., Brader, G., Pfaffenbichler, N. & Sessitsch, A. Next generation microbiome applications for crop production - limitations and the need of knowledge-based solutions. *Curr. Opin. Microbiol.* **49**, 59–65 (2019).
8. Busby, P. E. *et al.* Research priorities for harnessing plant microbiomes in sustainable

agriculture. *PLoS Biol.* **15**, 1–14 (2017).

9. Mitter, E. K., Tosi, M., Obregón, D., Dunfield, K. E. & Germida, J. J. Rethinking crop nutrition in times of modern microbiology: Innovative biofertilizer technologies. *Front. Sustain. Food Syst.* **5**, 1–23 (2021).

10. Timmusk, S., Behers, L., Muthoni, J., Muraya, A. & Aronsson, A. C. Perspectives and challenges of microbial application for crop improvement. *Front. Plant Sci.* **8**, 1–10 (2017).

11. Kaminsky, L. M., Trexler, R. V., Malik, R. J., Hockett, K. L. & Bell, T. H. The inherent conflicts in developing soil microbial inoculants. *Trends Biotechnol.* **37**, 140–151 (2019).

12. Hall-Stoodley, L., Costerton, J. W. & Stoodley, P. Bacterial biofilms: From the natural environment to infectious diseases. *Nat. Rev. Microbiol.* **2**, 95–108 (2004).

13. Monds, R. D. & O'Toole, G. A. The developmental model of microbial biofilms: ten years of a paradigm up for review. *Trends Microbiol.* **17**, 73–87 (2009).

14. Compant, S., Clément, C. & Sessitsch, A. Plant growth-promoting bacteria in the rhizo- and endosphere of plants: Their role, colonization, mechanisms involved and prospects for utilization. *Soil Biol. Biochem.* **42**, 669–678 (2010).

15. Pandin, C., Le Coq, D., Canette, A., Aymerich, S. & Briandet, R. Should the biofilm mode of life be taken into consideration for microbial biocontrol agents? *Microb. Biotechnol.* **10**, 719–734 (2017).

16. Elias, S. & Banin, E. Multi-species biofilms: Living with friendly neighbors. *FEMS Microbiol. Rev.* **36**, 990–1004 (2012).

17. Rendueles, O. & Ghigo, J. M. Multi-species biofilms: How to avoid unfriendly neighbors. *FEMS Microbiol. Rev.* **36**, 972–989 (2012).

18. Nadell, C. D., Drescher, K., Wingreen, N. S. & Bassler, B. L. Extracellular matrix structure governs invasion resistance in bacterial biofilms. *ISME J.* **9**, 1700–1709 (2015).

19. Morris, C. E. & Monier, J. M. The ecological significance of biofilm formation by plant-

644 associated bacteria. *Annu. Rev. Phytopathol.* **41**, 429–453 (2003).
645 20. Danhorn, T. & Fuqua, C. Biofilm formation by plant-associated bacteria. *Annu. Rev.*
646 *Microbiol.* **61**, 401–422 (2007).
647 21. Bakker, P. A. H. M. *et al.* The soil-borne identity and microbiome-assisted agriculture:
648 Looking back to the future. *Mol. Plant* **13**, 1394–1401 (2020).
649 22. Benz, J. & Meinhart, A. Antibacterial effector/immunity systems: It's just the tip of the
650 iceberg. *Curr. Opin. Microbiol.* **17**, 1–10 (2014).
651 23. Peterson, S. B., Bertolli, S. K. & Mougous, J. D. The central role of interbacterial
652 antagonism in bacterial life. *Curr. Biol.* **30**, 203–214 (2020).
653 24. Russell, A. B. *et al.* Type VI secretion delivers bacteriolytic effectors to target cells.
654 *Nature* **475**, 343–349 (2011).
655 25. García-Bayona, L., Guo, M. S. & Laub, M. T. Contact-dependent killing by *Caulobacter*
656 *crescentus* via cell surface-associated, glycine zipper proteins. *Elife* **6**, 1–26 (2017).
657 26. Souza, D. P. *et al.* Bacterial killing via a type IV secretion system. *Nat. Commun.* **6**, 1–
658 9 (2015).
659 27. Bernal, P., Allsopp, L. P., Filloux, A. & Llamas, M. A. The *Pseudomonas putida* T6SS
660 is a plant warden against phytopathogens. *ISME J.* **11**, 972–987 (2017).
661 28. Ahmad, S. *et al.* An interbacterial toxin inhibits target cell growth by synthesizing
662 (p)ppApp. *Nature* **575**, 674–678 (2019).
663 29. Whitney, J. C. *et al.* An interbacterial NAD(P)+ glycohydrolase toxin requires
664 elongation factor Tu for delivery to target cells. *Cell* **163**, 607–619 (2015).
665 30. Ting, S. Y. *et al.* Bifunctional immunity proteins protect bacteria against FtsZ-targeting
666 ADP-ribosylating toxins. *Cell* **175**, 1380–1392 (2018).
667 31. Klein, T. A., Ahmad, S. & Whitney, J. C. Contact-dependent interbacterial antagonism
668 mediated by protein secretion machines. *Trends Microbiol.* **28**, 387–400 (2020).
669 32. Yang, X., Long, M. & Shen, X. Effector–immunity pairs provide the T6SS
670 nanomachine its offensive and defensive capabilities. *Molecules* **23**, (2018).
671 33. Granato, E. T., Meiller-Legrand, T. A. & Foster, K. R. The evolution and ecology of

672 bacterial warfare. *Curr. Biol.* **29**, R521–R537 (2019).
673 34. Willett, J. L. E., Ruhe, Z. C., Goulding, C. W., Low, D. A. & Hayes, C. S. Contact-
674 dependent growth inhibition (CDI) and CdiB/CdiA two-partner secretion proteins. *J.*
675 *Mol. Biol.* **427**, 3754–3765 (2015).
676 35. Ruhe, Z. C., Low, D. A. & Hayes, C. S. Bacterial contact-dependent growth inhibition.
677 *Trends Microbiol.* **21**, 230–237 (2013).
678 36. Ho, B. T., Dong, T. G. & Mekalanos, J. J. A view to a kill: The bacterial type VI
679 secretion system. *Cell Host Microbe* **15**, 9–21 (2014).
680 37. Cianfanelli, F. R., Monlezun, L. & Coulthurst, S. J. Aim, load, fire: The type VI
681 secretion system, a bacterial nanoweapon. *Trends Microbiol.* **24**, 51–62 (2016).
682 38. Basler, M., Pilhofer, M., Henderson, G. P., Jensen, G. J. & Mekalanos, J. J. Type VI
683 secretion requires a dynamic contractile phage tail-like structure. *Nature* **483**, 182–186
684 (2012).
685 39. Backert, S., Grohmann, E. & (eds). *Type IV Secretion in Gram-Negative and Gram-*
686 *Positive Bacteria, Current Topics in Microbiology and Immunology*. (Springer, 2017).
687 40. Berger, K. H. & Isberg, R. R. Two distinct defects in intracellular growth complemented
688 by a single genetic locus in *Legionella pneumophila*. *Mol. Microbiol.* **7**, 7–19 (1993).
689 41. Brand, B. C., Sadosky, A. B. & Shuman, H. A. The *Legionella pneumophila icm* locus:
690 a set of genes required for intracellular multiplication in human macrophages. *Mol.*
691 *Microbiol.* **14**, 797–808 (1994).
692 42. Voth, D. E., Broederdorf, L. J. & Graham, J. Bacterial type IV secretion systems:
693 Versatile virulence machines. *Future Microbiol.* **7**, 241–257 (2012).
694 43. Christie, P. J. & Vogel, J. P. Bacterial type IV secretion: Conjugation systems adapted
695 to deliver effector molecules to host cells. *Trends Microbiol.* **8**, 354–360 (2000).
696 44. Hubber, A. & Roy, C. R. Modulation of host cell function by *Legionella pneumophila*
697 type IV effectors. *Annu. Rev. Cell Dev. Biol.* **26**, 261–283 (2010).
698 45. Steidle, A. *et al.* Identification and characterization of an N-acylhomoserine lactone-
699 dependent quorum-sensing system in *Pseudomonas putida* strain IsoF. *Appl. Environ.*

Microbiol. **68**, 6371–6382 (2002).

46. Steidle, A. *et al.* Visualization of N-acylhomoserine lactone-mediated cell-cell communication between bacteria colonizing the tomato rhizosphere. *Appl. Environ. Microbiol.* **67**, 5761–5770 (2001).

47. Espinosa-Urgel, M., Salido, A. & Ramos, J. L. Genetic analysis of functions involved in adhesion of *Pseudomonas putida* to seeds. *J. Bacteriol.* **182**, 2363–2369 (2000).

48. Kubori, T. & Nagai, H. The type IVB secretion system: An enigmatic chimera. *Curr. Opin. Microbiol.* **29**, 22–29 (2016).

49. Nagai, H. & Kubori, T. Type IVB secretion systems of *Legionella* and other Gram-negative bacteria. *Front. Microbiol.* **2**, 1–12 (2011).

50. Zatyka, M. & Thomas, C. M. Control of genes for conjugative transfer of plasmids and other mobile elements. *FEMS Microbiol. Rev.* **21**, 291–319 (1998).

51. Vincent, C. D. *et al.* Identification of the core transmembrane complex of the *Legionella* Dot/Icm type IV secretion system. *Mol. Microbiol.* **62**, 1278–1291 (2006).

52. Nakano, N., Kubori, T., Kinoshita, M., Imada, K. & Nagai, H. Crystal structure of Legionella DotD: Insights into the relationship between type IVB and type II/III secretion systems. *PLoS Pathog.* **6**, e1001129 (2010).

53. Yerushalmi, G., Zusman, T. & Segal, G. Additive effect on intracellular growth by *Legionella pneumophila* Icm/Dot proteins containing a lipobox motif. *Infect. Immun.* **73**, 7578–7587 (2005).

54. Liu, M. *et al.* ICEberg 2.0: An updated database of bacterial integrative and conjugative elements. *Nucleic Acids Res.* **47**, D660–D665 (2019).

55. Hood, R. D. *et al.* A Type VI secretion system of *Pseudomonas aeruginosa* targets a toxin to bacteria. *Cell Host Microbe* **7**, 25–37 (2010).

56. Pissaridou, P. *et al.* The *Pseudomonas aeruginosa* T6SS-VgrG1b spike is topped by a PAAR protein eliciting DNA damage to bacterial competitors. *Proc. Natl. Acad. Sci. U. S. A.* **115**, 12519–12524 (2018).

57. Liang, X. *et al.* An onboard checking mechanism ensures effector delivery of the type

VI secretion system in *Vibrio cholerae*. *Proc. Natl. Acad. Sci. U. S. A.* **116**, 23292–23298 (2019).

58. Dong, T. G., Ho, B. T., Yoder-Himes, D. R. & Mekalanos, J. J. Identification of T6SS-dependent effector and immunity proteins by Tn-seq in *Vibrio cholerae*. *Proc. Natl. Acad. Sci. U. S. A.* **110**, 2623–2628 (2013).

59. Nolan, L. M. *et al.* Identification of Tse8 as a Type VI secretion system toxin from Pseudomonas aeruginosa that targets the bacterial transamidosome to inhibit protein synthesis in prey cells. *Nat. Microbiol. 2021 69* **6**, 1199–1210 (2021).

60. Solaimanpour, S., Sarmiento, F. & Mrázek, J. Tn-seq explorer: A tool for analysis of high-throughput sequencing data of transposon mutant libraries. *PLoS One* **10**, 1–15 (2015).

61. Xue, H., Lozano-Durán, R. & Macho, A. P. Insights into the root invasion by the plant pathogenic bacterium *Ralstonia solanacearum*. *Plants* **9**, 1–9 (2020).

62. Lowe-Power, T. M., Khokhani, D. & Allen, C. How *Ralstonia solanacearum* exploits and thrives in the flowing plant xylem environment. *Trends Microbiol.* **26**, 929–942 (2018).

63. Bayer-Santos, E. *et al.* The opportunistic pathogen *Stenotrophomonas maltophilia* utilizes a type IV secretion system for interbacterial killing. *PLoS Pathog.* **15**, 1–29 (2019).

64. Harms, A. *et al.* A bacterial toxin-antitoxin module is the origin of inter-bacterial and inter-kingdom effectors of *Bartonella*. *PLoS Genet.* **13**, 1–22 (2017).

65. Sgro, G. G. *et al.* Bacteria-killing type IV secretion systems. *Front. Microbiol.* **10**, 1–20 (2019).

66. Qin, T., Zhou, H., Ren, H. & Liu, W. Distribution of secretion systems in the genus *Legionella* and its correlation with pathogenicity. *Front. Microbiol.* **8**, 1–12 (2017).

67. Basler, M. & Mekalanos, J. J. Type 6 secretion dynamics within and between bacterial cells. *Science* **337**, 815 (2012).

68. Ho, B. T., Basler, M., Mekalanos, J. J. & Ho, B., Basler, M., Mekalanos, J. Type 6

secretion system-mediated immunity to type 4 secretion system-mediated gene transfer. *Science* **342**, 250–253 (2013).

69. Basler, M., Ho, B. T. & Mekalanos, J. J. Tit-for-tat: Type VI secretion system counterattack during bacterial cell-cell interactions. *Cell* **152**, 884–894 (2013).

70. Stolle, A. S., Meader, B. T., Toska, J. & Mekalanos, J. J. Endogenous membrane stress induces T6SS activity in *Pseudomonas aeruginosa*. *Proc. Natl. Acad. Sci. U. S. A.* **118**, 1–12 (2021).

71. Spiewak, H. L. *et al. Burkholderia cenocepacia* utilizes a type VI secretion system for bacterial competition. *Microbiologyopen* **8**, e00774 (2019).

72. Chien, C. F. *et al.* HSI-II gene cluster of *Pseudomonas syringae* pv. tomato DC3000 encodes a functional type VI secretion system required for interbacterial competition. *Front. Microbiol.* **11**, 1118 (2020).

73. Molina-Santiago, C. *et al.* The extracellular matrix protects *Bacillus subtilis* colonies from *Pseudomonas* invasion and modulates plant co-colonization. *Nat. Commun.* **10**, 1–15 (2019).

74. Durán, D. *et al. Pseudomonas fluorescens* F113 type VI secretion systems mediate bacterial killing and adaption to the rhizosphere microbiome. *Sci. Rep.* **11**, 1–13 (2021).

75. Shyntum, D. Y. *et al.* The impact of type VI secretion system, bacteriocins and antibiotics on bacterial competition of *Pectobacterium carotovorum* subsp. brasiliense and the regulation of carbapenem biosynthesis by iron and the ferric-uptake regulator. *Front. Microbiol.* **10**, 2379 (2019).

76. Tian, Y. *et al.* Type VI secretion systems of *Erwinia amylovora* contribute to bacterial competition, virulence, and exopolysaccharide production. *Phytopathology* **107**, 654–661 (2017).

77. Schwarz, S. *et al. Burkholderia* type VI secretion systems have distinct roles in eukaryotic and bacterial cell interactions. *PLoS Pathog.* **6**, 77–78 (2010).

78. Nadell, C. D., Drescher, K. & Foster, K. R. Spatial structure, cooperation and

competition in biofilms. *Nat. Rev. Microbiol.* **14**, 589–600 (2016).

79. Hibbing, M. E., Fuqua, C., Parsek, M. R. & Peterson, S. B. Bacterial competition: Surviving and thriving in the microbial jungle. *Nat. Rev. Microbiol.* **8**, 15–25 (2010).

80. Pandit, A., Adholeya, A., Cahill, D., Brau, L. & Kochar, M. Microbial biofilms in nature: unlocking their potential for agricultural applications. *J. Appl. Microbiol.* **129**, 199–211 (2020).

81. Krishna Kumar, R. *et al.* Droplet printing reveals the importance of micron-scale structure for bacterial ecology. *Nat. Commun.* **12**, 1–12 (2021).

82. Kuiper, I. *et al.* Characterization of two *Pseudomonas putida* lipopeptide biosurfactants, putisolvin I and II, which inhibit biofilm formation and break down existing biofilms. *Mol. Microbiol.* **51**, 97–113 (2004).

83. Gotschlich, A. *et al.* Synthesis of multiple N-acylhomoserine lactones is wide-spread among the members of the *Burkholderia cepacia* complex. *Syst. Appl. Microbiol.* **24**, 1–14 (2001).

84. Zhang, R., Vivanco, J. M. & Shen, Q. The unseen rhizosphere root–soil–microbe interactions for crop production. *Curr. Opin. Microbiol.* **37**, 8–14 (2017).

85. Clark, D. J. & Maaløe, O. DNA replication and the division cycle in *Escherichia coli*. *J. Mol. Biol.* **23**, 99–112 (1967).

86. Lambertsen, L., Sternberg, C. & Molin, S. Mini-Tn7 transposons for site-specific tagging of bacteria with fluorescent proteins. *Environ. Microbiol.* **6**, 726–732 (2004).

87. Choi, K.-H. & Schweizer, H. P. Mini-Tn7 insertion in bacteria with single attTn7 sites: example Pseudomonas aeruginosa. *Nat. Protoc.* **1**, 153–161 (2006).

88. Aguilar, C., Schmid, N., Lardi, M., Pessi, G. & Eberl, L. The lclR-family regulator BapR controls biofilm formation in *B. cenocepacia* H111. *PLoS One* **9**, 1–7 (2014).

89. Huber, B. *et al.* Genetic analysis of functions involved in the late stages of biofilm development in *Burkholderia cepacia* H111. *Mol. Microbiol.* **46**, 411–426 (2002).

90. de Lorenzo, V. & Timmis, K. N. Analysis and construction of stable phenotypes in gram-negative bacteria with Tn5- and Tn10-derived minitransposons. *Methods*

Enzymol. **235**, 386–405 (1994).

91. Schneider, C. A., Rasband, W. S. & Eliceiri, K. W. NIH Image to ImageJ: 25 years of image analysis. *Nat. Methods* **9**, 671–675 (2012).

92. Flannagan, R. S., Linn, T. & Valvano, M. A. A system for the construction of targeted unmarked gene deletions in the genus *Burkholderia*. *Environ. Microbiol.* **10**, 1652–1660 (2008).

93. Darling, A. C. E., Mau, B., Blattner, F. R. & Perna, N. T. Mauve: Multiple alignment of conserved genomic sequence with rearrangements. *Genome Res.* **14**, 1394–1403 (2004).

94. Medema, M. H., Takano, E. & Breitling, R. Detecting sequence homology at the gene cluster level with MultiGeneBlast. *Mol. Biol. Evol.* **30**, 1218–1223 (2013).

95. Gallagher, L. A., Shendure, J. & Manoil, C. Genome-scale identification of resistance functions in *Pseudomonas aeruginosa* using Tn-seq. *MBio* **2**, 1–8 (2011).

96. Higgins, S., Gualdi, S., Pinto-Carbó, M. & Eberl, L. Copper resistance genes of *Burkholderia cenocepacia* H111 identified by transposon sequencing. *Environ. Microbiol. Rep.* **12**, 241–249 (2020).

97. Bolger, A. M., Lohse, M. & Usadel, B. Trimmomatic: A flexible trimmer for Illumina sequence data. *Bioinformatics* **30**, 2114–2120 (2014).

98. Martin, M. Cutadapt removes adapter sequences from high-throught sequencing reads. *EMBnet.journal* **17**, (2011).

99. Langmead, B. & Salzberg, S. L. Fast gapped-read alignment with Bowtie 2. *Nat. Methods* **9**, 357–359 (2012).

100. Christensen, B. B. *et al.* Molecular tools for study of biofilm physiology. *Methods Enzymol.* **310**, 20–42 (1999).

101. Heydorn, A. *et al.* Experimental reproducibility in flow-chamber biofilms. *Microbiology* **146**, 2409–2415 (2000).

102. Bulgarelli, D. *et al.* Revealing structure and assembly cues for *Arabidopsis* root-inhabiting bacterial microbiota. *Nature* **488**, 91–95 (2012).

103. Schindelin, J. *et al.* Fiji: An open-source platform for biological-image analysis. *Nat. Methods* **9**, 676–682 (2012).
104. Liang, Y. *et al.* A nondestructive method to estimate the chlorophyll content of *Arabidopsis* seedlings. *Plant Methods* **13**, 1–10 (2017).
105. Lichtenthaler, H. K. & Wellburn, A. R. Determinations of total carotenoids and chlorophylls a and b of leaf extracts in different solvents. *Biochem. Soc. Trans.* **11**, 591–592 (1983).
106. Chetrit, D., Hu, B., Christie, P. J., Roy, C. R. & Liu, J. A unique cytoplasmic ATPase complex defines the *Legionella pneumophila* type IV secretion channel. *Nat. Microbiol.* **3**, 678–686 (2018).

Acknowledgments

This work was funded in part by the Swiss National Science Foundation grants CRSII5_186410 and 310030_192800. We would like to thank Claudio Aguilar for his assistance in constructing the IsoF mini-Tn*5* library and Alessandra Vitale for help with the TnSeq. We would like to thank Carlotta Fabbri, Joel Steger and Elina Leu for technical support. We are grateful to Yi-chi Chen and Stefano Gualdi for helpful discussions and Kirsty Agnoli for improving the English.

Author contributions

GP-M, GC-O and LE designed the overall experimental plan for the manuscript. GP-M performed the majority of the experiments presented and wrote the manuscript with input from all authors. GC-O contributed to project management and performed the Tn*5* library experiments, the initial bacterial competition experiments and the flow cell biofilm experiments with the wild type strains. MP-C contributed to the analysis of the TnSeq library, bioinformatic analyses, and the sequencing and annotation of the genome of IsoF. KA supported all molecular microbiology experiments and contributed to writing the manuscript. AB contributed to the design of the plant experiment and performed the principal component analysis,

hierarchical clustering and related analyses. LE contributed to project management and to writing the manuscript. **Competing interests:** The authors declare no competing interests.

Figures

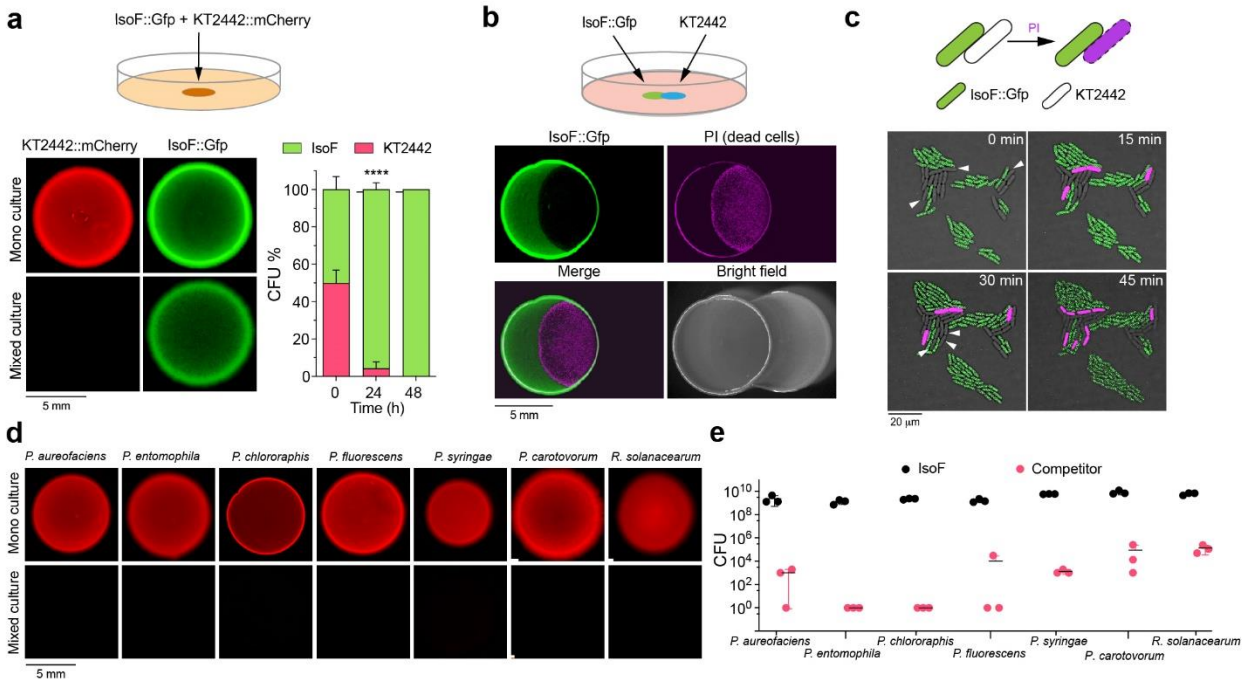

Figure 1. IsoF displays contact-dependent antagonism against a wide range of Gram-negative bacteria a, IsoF::Gfp outcompetes KT2442::mCherry after co-inoculation on ABC agar plates. Fluorescence is indicative of viable bacteria. The percentage of the CFUs of each bacterial population in the mixed culture at 0 h, 24 h, and 48 h is shown. Data are mean ± s.d. from 3 biological replicates (n=3). Unpaired t-test, ****$P < 0.0001$. **b**, IsoF antagonism is restricted to areas where IsoF::Gfp and KT2442 colonies are in direct contact. The medium was supplemented with propidium iodide (PI) to visualize dead cells. **c**, IsoF::Gfp kills KT2442 cells in a contact-dependent manner. Cell death was monitored by PI staining (cells shown in magenta). **d**, IsoF kills a wide range of Gram-negative plant-associated bacteria, including *P. aureofaciens, P. entomophila, P. chlororaphis, P. fluorescens, P. syringae, P. carotovorum,* and *R. solanacearum*. All competitors were tagged with mCherry. **e**, CFUs were determined after 24 h of competition. Data are mean ± s.d. from 3 independent biological replicates (n=3).

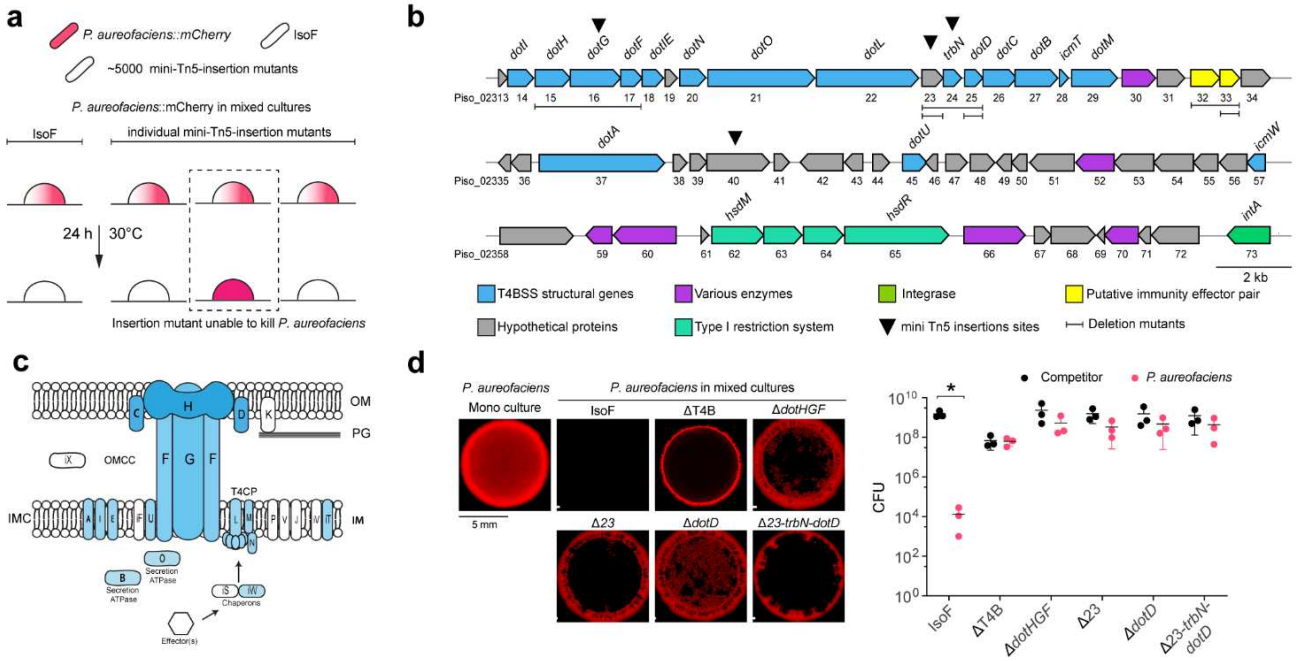

Figure 2. The IsoF T4BSS-dependent killing machine is encoded on a genomic island (GI). **a**, Single IsoF-Tn*5*-insertion mutants were mixed with *P. aureofaciens* tagged with mCherry. Red fluorescence indicates the loss of killing activity by the mutant. **b**, Genetic organization of the IsoF GI that encodes a T4BSS required for bacterial killing. The cluster has a length of 69.9 kb and codes for 17 T4BSS structural and 34 hypothetical proteins. Additionally, the 3' end encodes a Type I RM system and an integrase. Regions that were deleted in defined mutants are underlined in black: Δ*dotHGF,* Δ23, Δ*dotD*, Δ23-*trbN-dotD*, Δ33, and Δ32-33. **c**, Architecture of the T4BSS gene cluster in *Legionella*. Homologs of proteins highlighted in blue are encoded by the IsoF-GI. In the *Legionella* Icm/Dot system, effector molecules bind to chaperons which interact with the type 4 coupling protein (T4CP) before the effector molecules are translocated through the outer membrane core complex. The two ATPases provide energy and interact with the inner membrane complex (IMC) at the substrate recognition and translocation domains (modified from[39,106]). **d**, Fluorescence images show *P. aureofaciens*::mCherry in competition with the IsoF wild type and various deletion mutants after 24 h of co-incubation. CFUs of the two competing strains. Data are mean ± s.d. of three independent biological replicates (n=3). Unpaired t-test, $*P < 0.05$.

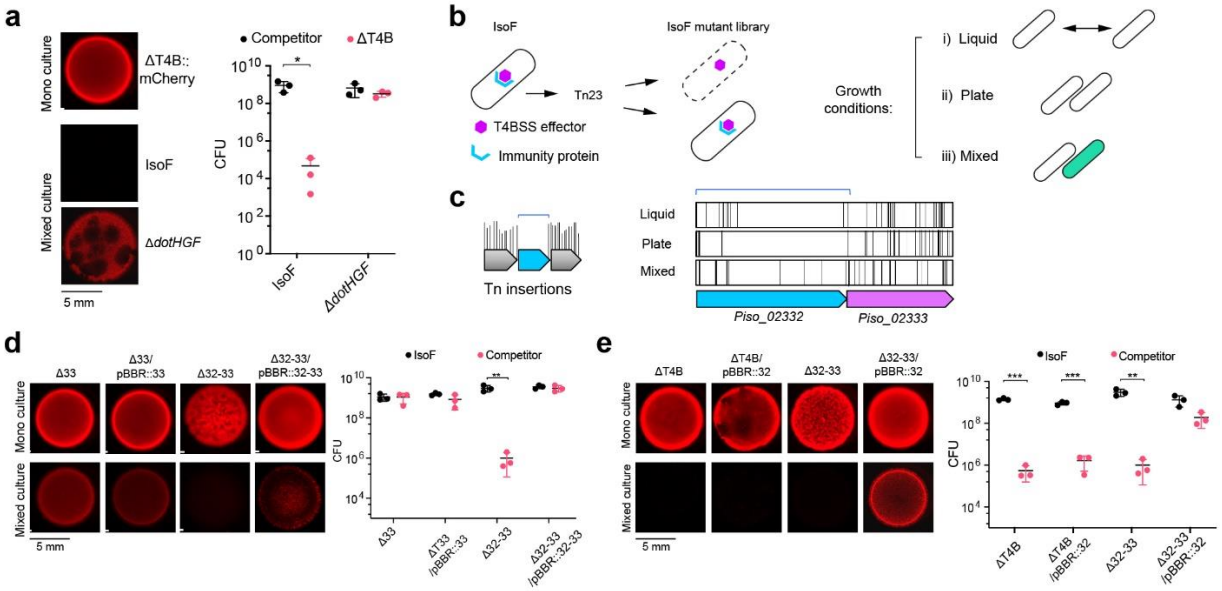

Figure 3. An E-I pair is encoded within the *kib* gene cluster. a, Contact-dependent competition of the ΔT4B mutant against the IsoF wild type and the Δ*dotHGF* deletion mutant. Representative fluorescence images of three independent experiments are shown. **b**, An effector will be toxic for the cell in the absence of its cognate immunity protein. The following conditions were used to challenge an IsoF Tn*23* mutant library: (i) growth in liquid medium with shaking to prevent cell-to-cell contact, (ii) growth on an agar surface either alone or (iii) in the presence of the competitor *P. aureofaciens* to promote competition (mixed). **c**, The unique insertion density approach of the Tn-Seq explorer software was used to identify genes that provide a fitness benefit for growth under the applied growth conditions[60]. *Piso_02332* (blue) was found to have very few transposon insertions under all three culture conditions. A putative effector gene, *Piso_02333* (magenta), is located downstream of *Piso_02332*. The Tn*23* insertions in the two genes for the three growth conditions are shown. **d**, CDC of IsoF against the deletion mutants Δ32-33 (lacking the E-I pair). Δ33 (lacking the effector gene) and their complemented derivatives. **e**, CDC of the IsoF wild type against mutants ΔT4B/pBBR::32 and Δ32-33/pBBR::32. Representative fluorescence images of three independent experiments are shown. CFUs of the competing strains were determined after 24 h incubation. Data are mean ± s.d. of three independent replicates (n=3). Unpaired t-test, $*P < 0.05$; $**P < 0.01$; $***P < 0.001$.

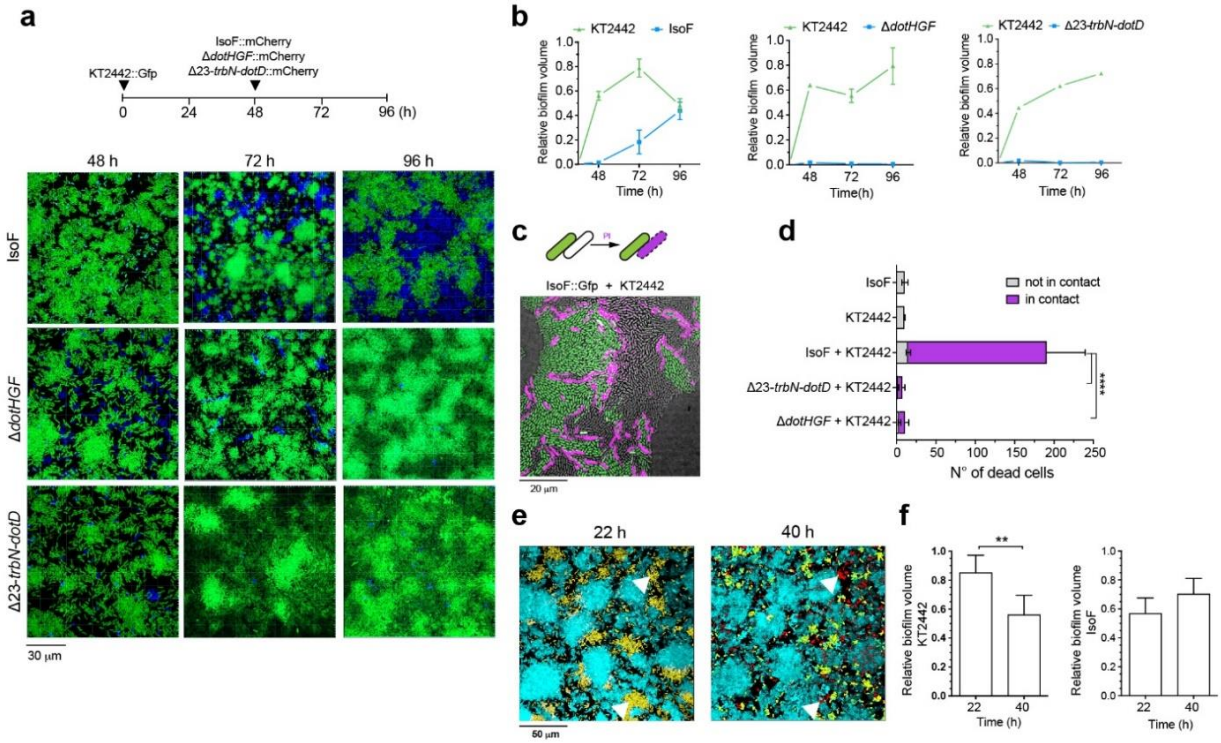

Figure 4. IsoF wild type invades and displaces a pre-established KT2442 biofilm. a, A two day-old biofilm of KT2442::Gfp (green) is invaded by IsoF::mCherry (blue) but not by Δ*dotHGF*::mCherry (blue) or Δ23-*trbN*-*dotD*::mCherry (blue). **b**, Relative biofilm biomass (volume) of KT2442::Gfp relative to IsoF::mCherry, Δ*dotHGF*::mCherry and Δ23-*trbN*-*dotD*::mCherry. Data are mean ± s.d. from up to three biological replicates (n=3). **c**, Competition of IsoF::Gfp against KT2442 after 18 h of incubation. Dead cells (magenta) were visualized by staining with PI. **d**, The number of dead cells in contact and not in contact with a green fluorescent cell were quantified from at least 9 randomly chosen images from the different competition experiments. As a control, the strains were also inoculated without a competitor and the number of dead cells was determined. Data are mean ± s.d. of three independent replicates (n=3). Unpaired t-test, **** $P < 0.0001$. **e**, Mixed biofilm of KT2442::Gfp (yellow) and IsoF::Cfp (cyan) after 40 h of co-cultivation. Dead cells (red) were visualized by staining with PI. **f**, Relative biofilm volumes of KT2442 and IsoF at 22 and 40 h. Unpaired t-test, ** $P < 0.01$.

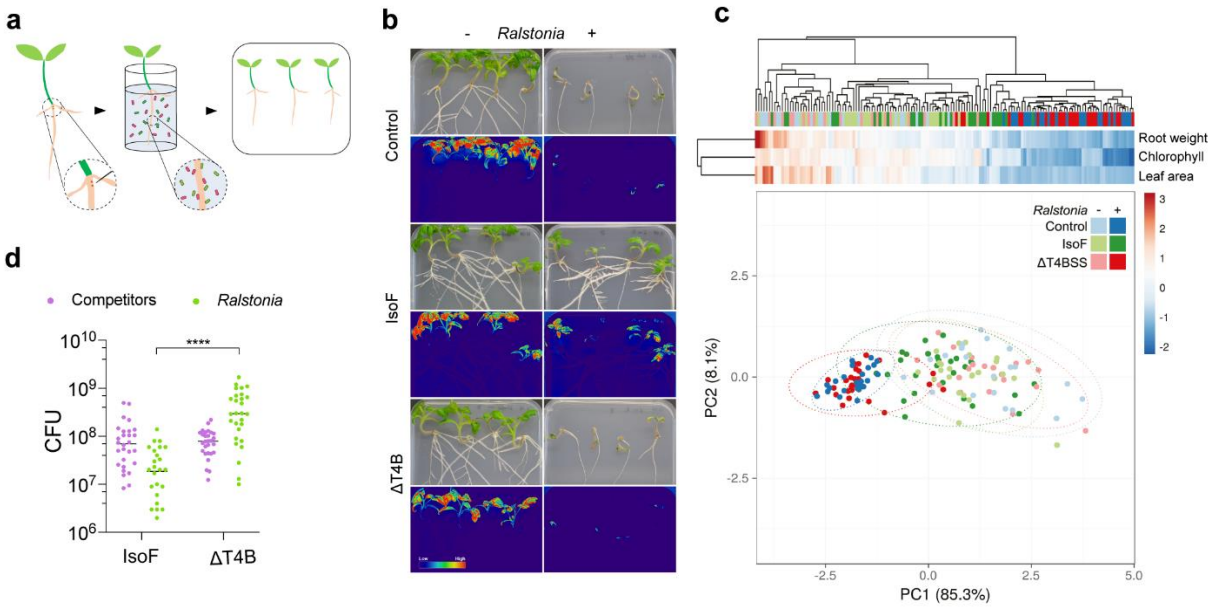

Figure 5. IsoF-T4BSS protects tomato plants against bacterial wilt. a, Schematic representation of the experimental approach used. Seedlings were injured twice with a needle in the root-shoot junction and immersed in the bacterial suspensions. Inoculated seedlings were transferred to ½ MS plates for further growth. **b**, Representative images of tomato plants 22 days after inoculation. False color pictures display the green component of the RGB pictures to estimate chlorophyll content. **c**, Principal component analysis and hierarchical clustering heatmap of estimated plant health parameters. **d**, CFUs of recovered bacterial competitor cells from the tomato roots. In total 28 plants were assessed with a minimum of 8 plants per treatment for each of the three independent replicates (n=3). Unpaired t-test, $^{****}P < 0.0001$.

Supplementary Files

This is a list of supplementary files associated with this preprint. Click to download.

- SupplementaryInformation.pdf
- ExtendedData.pdf
- ExtendedDataVideo1medium.mp4